Available online at www.sciencedirect.com
ScienceDirect
Polymer 48 (2007) 4874–4882
polymer
www.elsevier.com/locate/polymer

# Transcrystalline structures of poly(L-lactide)

Naoya Ninomiya, Kensuke Kato, Atsuhiro Fujimori*, Toru Masuko

*Graduate School of Science and Engineering, Yamagata University, Jonan 4-3-16, Yonezawa, Yamagata 992-8510, Japan*

Received 1 December 2006; received in revised form 30 May 2007; accepted 3 June 2007
Available online 13 June 2007

**Abstract**

Poly(L-lactide) (PLLA) film containing transcrystalline (TC) structures can easily be obtained by placing PLLA films melted between two poly(tetrafluoroethylene) (PTFE) sheets, followed by isothermal crystallization at 122 °C. The fine structures of the PLLA-TC film were studied by various structural techniques such as X-ray diffractometry, optical microscopy and transmission electron microscopy. We also examined the purification effect upon the morphology of PLLA-TC film. The formation of the TC structures revealed that one-dimensional spherulitic growth occurred from the assembling impurities as nucleation agent near the PTFE substrate in the heterogeneous nucleation system. We found that the *b*-axis of PLLA crystal was parallel to the lamellae growth direction confirmed using X-ray diffraction. The precipitated PLLA film crystallized in a similar process exhibited scanty TC textures, suggesting that the existence of impurity in the PLLA sample was an important factor for the formation of those structures.


*Keywords:* Poly(L-lactide); Transcrystalline structure; Heterogeneous nucleation

## 1. Introduction

When crystalline polymers such as polypropylene (PP) [1–6], poly(etheretherketone) (PEEK) [7–9] and nylon-6 [10] are crystallized from their melt state, transcrystalline (TC) textures are formed by predominant nucleation initiating on the substrate. In those textures, lamellae growths are restricted spatially and the TC textures resulted exhibit regularly oriented morphology perpendicular to the substrate.

The principle factors for the formation of TC layers on the substrate include both the surface properties of substrates [4,5,11–16] and the suitable crystallization conditions [16–18]. In particular, exterior properties such as the surface topology and the surface free energy of substrate are the most important factors for controlling the transcrystallization on the substrate's surface. Hata et al. [5] have reported that PP forms TC layers on the sheet of poly(tetrafluoroethylene) (PTFE), while only spherulitic textures of the polymer are observed on other substrates coated with metal vapor. Their conclusion is that the TC layers formation is independent of the substrate species or difference in their surface energy, but is strongly governed by geometrical surface morphology or surface roughness.

Poly(L-lactide) (PLLA) is one of the biodegradable and biocompatible aliphatic polyesters, which is widely expected to be available for surgical suture [19–21] and drug delivery systems [22]. So far, several investigators have already described its crystal structures, morphology of solution-grown crystals and the kinetics of spherulitic crystallization. The crystal of PLLA exhibits polymorphism known as the α-form [23–25] and the β-form [23,26,27]. Examinations concerned with the crystallization behavior of PLLA have been published by several investigators [28–30]. Vasanthakumari–Pennings [28] and Miyata–Masuko [30] demonstrated the relationship between structural features and crystallization conditions under the isothermal or non-isothermal processes. Recently, the orientation of PLLA crystal perpendicular to the film surface has been reported to be available for piezoelectric materials

* Corresponding author. Tel./fax: +81 0238 26 3073.
*E-mail address:* fujimori@yz.yamagata-u.ac.jp (A. Fujimori).

0032-3861/$ - see front matter © 2007 Elsevier Ltd. All rights reserved.
doi:10.1016/j.polymer.2007.06.012

[31–33]. However, the fine structures of the transcrystalline (TC) film of PLLA have scarcely been studied until now.

In this paper, we will characterize structurally the TC layers of PLLA films prepared on PTFE substrates. The suitable transcrystallization condition of the polymer will be examined by various structural techniques such as X-ray diffractometry, optical microscopy and transmission electron microscopy.

## 2. Experimental

### 2.1. Materials

A high L-content (>99%) commercial grade PLLA pellets (kindly supplied by Unitika Co., Ltd, Japan) were utilized mainly without any reprecipitation process. For comparison, purified PLLA samples were prepared by the process where the pellets were dissolved in chloroform and then the polymer was reprecipitated repeatedly from a large quantity of methanol at room temperature. As-received and reprecipitated PLLA samples were abbreviated as sample A and sample B, respectively. Molecular characterization of the PLLA samples was carried out on a JASCO 860-CO gel permeation chromatograph using tetrahydrofuran carrier at 40 °C with a flow rate of 1 ml $min^{-1}$. Standard polystyrene was used for molecular weight calibration. The sample showed weight-average molecular weight ($M_w$) = $2.0 \times 10^5$ and the polydispersity index ($M_w/M_n$) = 1.94; there was no substantial difference in the weight-average molecular weight before and after the reprecipitation.

### 2.2. Preparation of PLLA-TC film

A suitable amount of the samples A and B was sandwiched between two PTFE sheets (Dupont Co.) of 0.5 mm thickness as spacers for preparing TC films of almost the same thickness. The sandwiched PLLA was melted at 200 °C for 10 min in a hot press; then the press temperature was gradually decreased to a programmed crystallization temperature ($T_c$) and kept isothermally for 3 h. After the crystallization, the sandwiched sample was quenched into ice water. The $T_c$s were changed in the range from 114 °C to 130 °C. A schematic illustration of this preparation method is shown in Fig. 1.

### 2.3. Polarized optical microscopy

Thin samples of 20 μm thickness were cut from the crystallized films using a Reichert ultramicrotome equipped with a glass knife. The morphological texture of these thin pieces was examined by use of an Olympus BH-2 polarizing microscope equipped with a video camera system. A Linkam THM-600 hot-stage was also utilized to measure the spherulite or TC growth rates. In these kinetic experiments, the samples prepared by a similar method described above were first melted at 200 °C for 10 min, cooled down rapidly to programmed $T_c$s, and then at those temperatures kept isothermally for enough time.

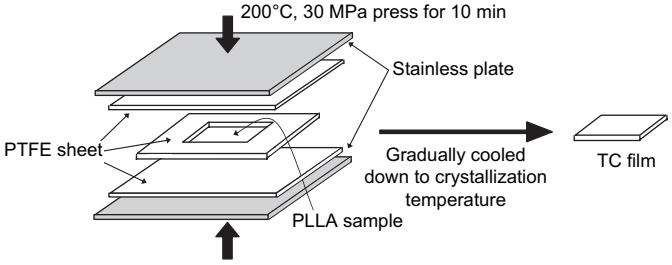


Fig. 1. Schematic illustration of PLLA-TC film preparation method used in this study.

### 2.4. Differential scanning calorimetry (DSC)

Thermal analysis for the bulk TC films was carried out using a Perkin–Elmer Pyris 1 DSC at a heating rate of 10 °C $min^{-1}$ under nitrogen atmosphere. The sample weight was around 5 mg and the DSC traces were calibrated with indium and zinc standards before the measurements.

### 2.5. X-ray measurements for the samples

Wide-angle X-ray diffraction (WAXD) measurements for the bulk PLLA-TC films were performed by use of a Rigaku R-AXIS diffractometer operated at 45 kV and 200 mA. The WAXD photographs of the samples were taken at room temperature using graphite-monochromatized Cu Kα radiation ($\lambda = 1.542$ Å) focused through a 0.8 mm pinhole collimator. A cylindrical imaging plate detector was used for recording diffraction patterns.

To obtain long periods of the TC films, small angle X-ray scattering (SAXS) experiments were carried out on an MAC Science M18XHF apparatus consisting of an 18 kW rotating-anode X-ray generator with a Cu target (wavelength, $\lambda = 1.5418$ Å) operated at 50 kV and 300 mA. This apparatus was equipped with a pyrographite monochromator, a pinhole collimation system ($\phi \sim 0.3$ mm, 0.3 mm, 1.1 mm), a vacuum chamber for the scattered beam path, and a two-dimensional imaging plate detector system (DIP-220).

### 2.6. Transmission electron microscopy (TEM)

The fracture surface (cross-section view) of the bulk TC samples was examined with a Philips CM-300 transmission electron microscope operated at an accelerating voltage of 200 kV. A two-step replica technique was utilized for the fractured samples, where a thin cellulose acetate (CA) film wetted with small amount of methyl acetate (MA) solvent (99.5%, Kanto Kagaku Reagent Co. Ltd) was forced to contact with the sample fracture surface in order to produce an adequate replica. The replica was then stripped from the sample and shadowed with Au/Pd alloy at an oblique angle of 30°. After carbon coating and dissolving the CA film by MA, the metal-shadowed replica sample was transferred onto TEM grids.

## 3. Results and discussion

### 3.1. Formation of PLLA-TC film with PTFE substrate

Fig. 2 shows the optical micrographs of the as-received PLLA-TC thin films at various $T_c$s. Well-organized TC structures can be observed only in the case at $T_c = 122\,^{\circ}C$ (see Fig. 2b), although spherulitic entities inevitably appear in other isothermal crystallization conditions. Additionally, heterogeneous nuclei exist on the PTFE surface with a relatively constant distance. In other words, the PTFE surface apparently plays a role in a kind of nucleating agent for isothermal crystallization of the PLLA films. The difference in observed PLLA-TC structures is mainly governed by both the growth rate of spherulite and the density of heterogeneous nuclei in each $T_c$.

The TC structures observed are composed of two-dimensional alignments of slender, columnar spherulites (something like a cucumber shape), which develop to crystallize on the PTFE sheets. The crystallization mode seems to be one-dimensional and heterogeneous. When we rotate clockwise the TC sample on a revolving stage (the thickness direction is tangential to rotation), the yellow color of the sample at the $-45^{\circ}$ diagonal position changes to the blue at $+45^{\circ}$ position, which indicates the TC samples to be negative birefringent. Thus, the *c*-axis of the PLLA unit cell is anticipated as lying in parallel to the film surface.

The spherulite growth rates ($G$) for samples A and B are shown in Fig. 3 as a function of $T_c$, where the former has indicated maximum value at $T_c = 122\,^{\circ}C$. The averaged diameter of the TC in the center of the film, where sometimes ordinary spherulitic crystallization happens, changes with $T_c$, as illustrated in Fig. 2. The TC film in the case at $T_c = 114\,^{\circ}C$ contains both the TC layers and the spherulites, indicating that the latter developed the center of the film before the former completely grew up from the interfaces of both sides of PTFE sheet. On the other hand, the TC film in higher $T_c$ ($= 130\,^{\circ}C$) exhibited ambiguous boundary of TC layers. This morphology resulted from disordered orientation of the PLLA lamellae, which might be caused by the lamellar growth free from spatial restriction with relatively slow growth rate.

Fig. 4 shows the DSC heating traces of the TC film obtained at various isothermal crystallization temperatures ($T_c$s). The crystallization peak is not observed in all the films since their crystallizable amorphous region scarcely exists in the process of crystallization. Obviously, from these DSC heating traces, the glass transition temperature ($T_g$) and the peak of melting point ($T_m$) locate around $63\,^{\circ}C$ and $165\,^{\circ}C$, respectively, are summarized in Table 1. According to Eq. (1), the crystallinity ($\chi_c$) value of each TC film was calculated using the endothermic enthalpy change ($\Delta H_m$) values.

$$\chi_c = \frac{\Delta H_m}{\Delta H_m^0} \times 100 \qquad (1)$$

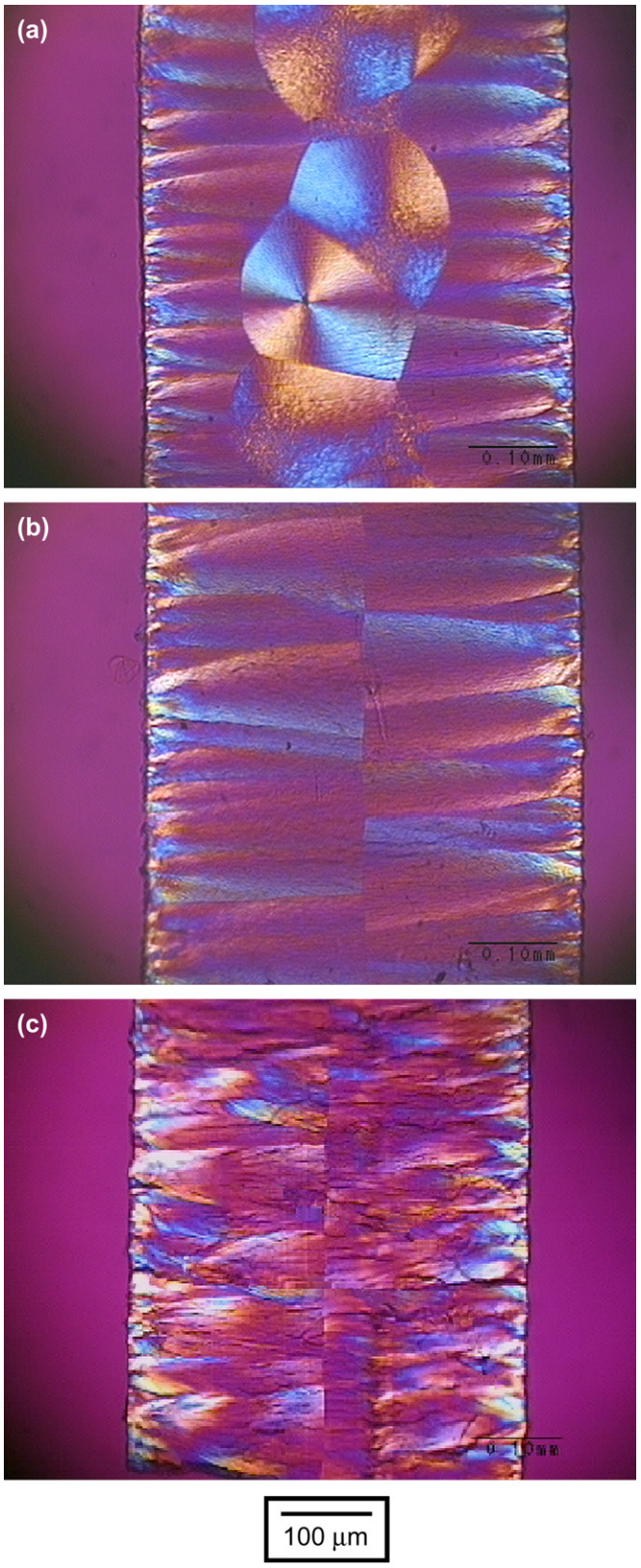


Fig. 2. Polarized optical micrographs of the as-received PLLA-TC thin films at various isothermal crystallization temperatures in the edge direction: (a) $T_c = 114\,^{\circ}C$; (b) $T_c = 122\,^{\circ}C$; (c) $T_c = 130\,^{\circ}C$.

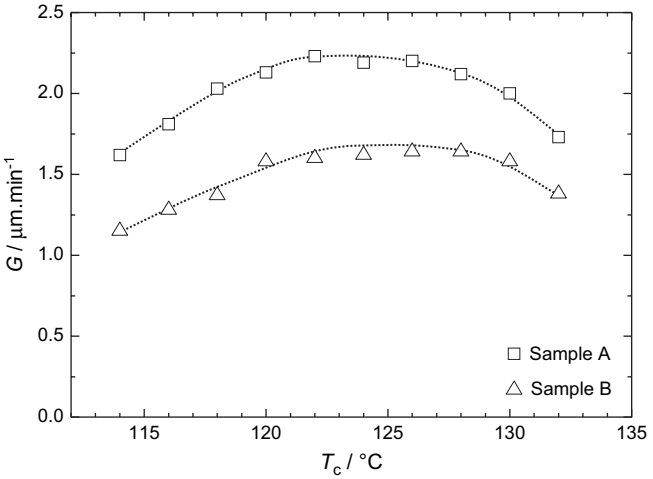


Fig. 3. Spherulite growth rate, $G$ (μm min$^{-1}$), as a function of isothermal crystallization temperature for the samples A and B.

Here, $\Delta H_m^0$ is the value of 135 J g$^{-1}$ for the melting enthalpy of 100% crystalline PLLA [30]. The $\chi_c$ and $\Delta H_m$ values of each TC film also are listed in Table 1.

We find that the peak position of melting temperature shifts to the high temperature region with an increase in $T_c$ value.

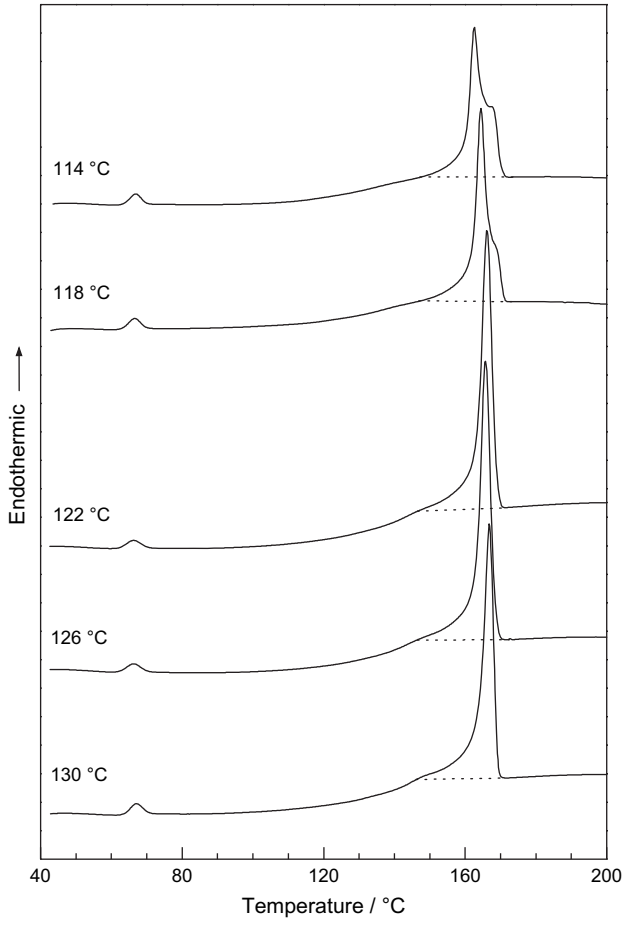


Fig. 4. DSC traces of 1st heating for the TC films obtained at various isothermal crystallization temperatures.

Table 1
Thermodynamic parameters of the PLLA-TC at various $T_c$s measured from DSC thermograms

| $T_c$/°C | $T_g$/°C | Peak of melting point/°C | $\Delta H$/J g$^{-1}$ ($\chi_c$/%) |
|---|---|---|---|
| 114 | 63.6 | 162.6 | 40.0 (29.6) |
| 118 | 63.0 | 164.5 | 42.5 (31.4) |
| 122 | 62.8 | 166.1 | 52.3 (38.7) |
| 126 | 62.9 | 165.8 | 52.6 (39.0) |
| 130 | 63.8 | 166.8 | 48.3 (35.7) |

The findings imply that the lamellar thickening is induced by the increase of $T_c$. Therefore, two melting peaks are observed in the TC film at $T_c = 114$ °C arising from different lamellae thicknesses caused by isothermal crystallization temperature. The sample crystallized at 118 °C shows similar melting behavior. The well-organized TC film at $T_c = 122$ °C exhibits an increased $\chi_c$ value as compared with that of the other TC film at lower $T_c$. The results suggest that the formation of closely packed crystallites in the TC film at $T_c = 122$ °C yields few isolated spherulites.

### 3.2. Fine structure of PLLA-TC regions

As mentioned above, the PLLA-TC film without any isolated spherulite structure can be obtained by suitable crystallization conditions on PTFE substrates. The polarized optical micrographs of the PLLA-TC film in the through direction are shown in Fig. 5. These photographs represent the through views in the depth at (a) 80 μm, (b) 120 μm, (c) 160 μm and (d) 200 μm in distance from the film surface. For the region close to the film surface (Fig. 5a), the boundary of individual crystallites cannot be clearly distinguished, implying that those crystallites grown from a large number of nuclei exist in the interfacial region between PLLA and PTFE. On the other hand, we find the crystallites like a spherulitic texture in the central region of the film (Fig. 5b and c). Additionally, it is apparent that the size of spherulites becomes large with increasing distance from the film surface. The average size of the spherulite is about 120 μm in diameter, corresponding to width of fibril in parallel to edge direction, as seen in Fig. 2b. In Fig. 5d, the other crystallites are observed at a different place from the former. Those newly appearing crystallites suggest that the TC layers were grown on another film surface.

The orientation of lamellae in the TC regions was examined by X-ray diffraction. Fig. 6 displays the WAXD photographs of the PLLA-TC film in the (a) edge and (b) through directions. The through-view WAXD photographs of the film show that the diffraction patterns are to be Debye rings due to randomly oriented PLLA crystallites. On the other hand, fiber diagrams are observed when the X-ray beam was irradiated to the edge direction of the films. These WAXD patterns indicate that the PLLA crystallites exist in TC layers oriented parallel to the film surface. From the fiber diagram, the reciprocal lattice for the $a^*-c^*$ and $b^*-c^*$ nets based on lattice constants for PLLA α-form ($a = 10.8$ Å, $b = 6.04$ Å,

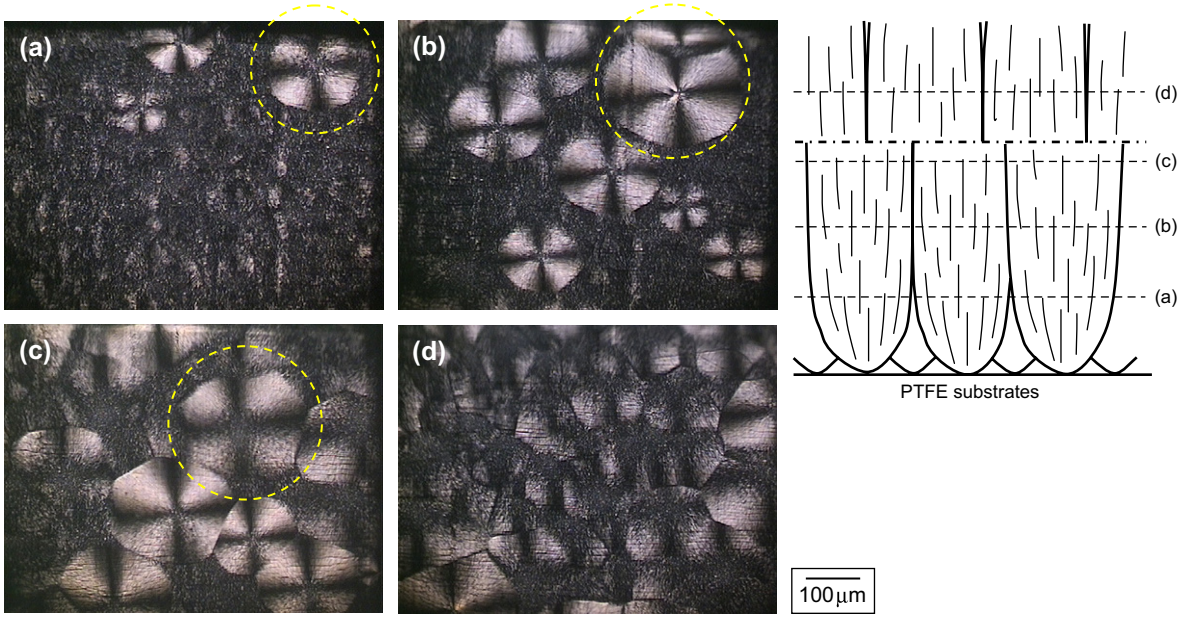


Fig. 5. Polarized optical micrographs of the PLLA-TC film obtained at $T_c = 122$ °C in the through view: (a) 80 μm; (b) 120 μm; (c) 160 μm; (d) 200 μm.

$c = 28.7$ Å, orthorhombic [25]) is shown in Fig. 7. Interestingly, the reflection on (110), (210) and (113) planes appears clearly compared with the other reflections, suggesting that the growth direction of TC lies in parallel to the *b*-axis. The indexing results for all the reflections are summarized in Table 2. Fig. 8 shows the lamellar growth model of the PLLA-TC

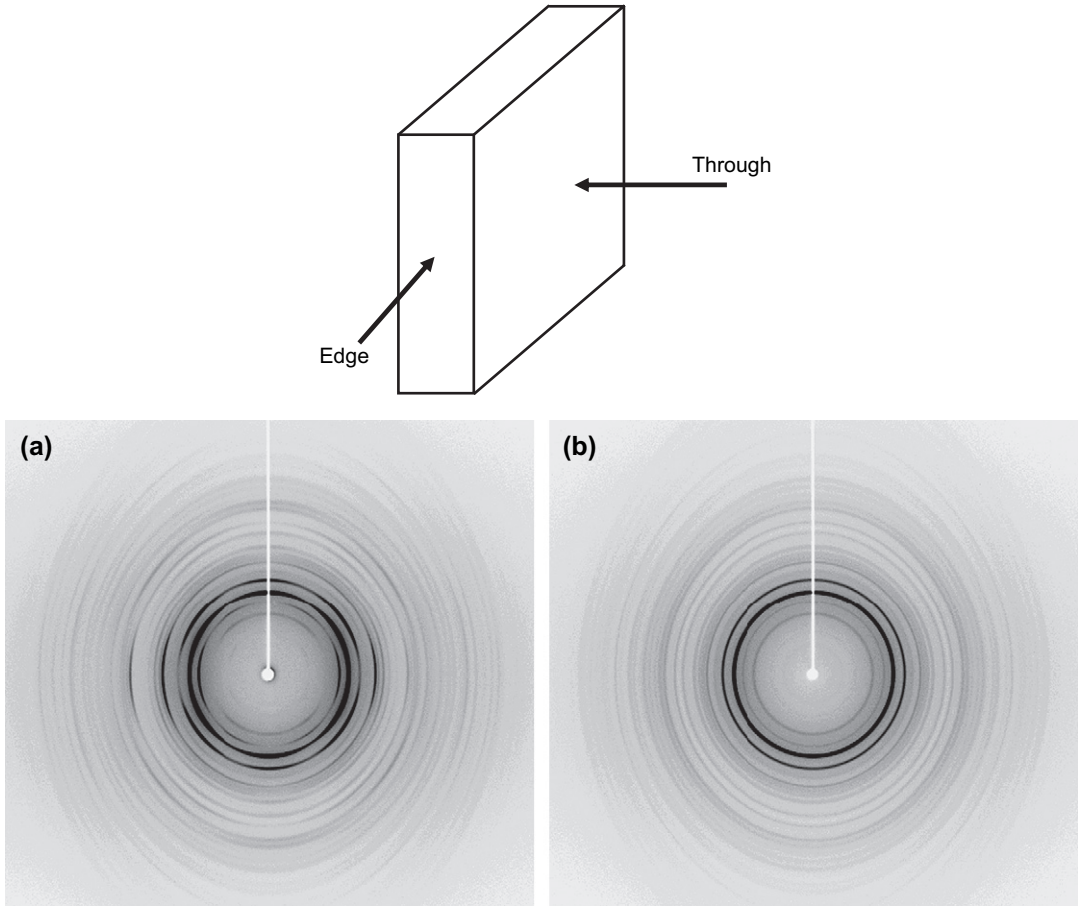


Fig. 6. WAXD photographs of the PLLA-TC film obtained at $T_c = 122$ °C in the (a) edge- and (b) through direction.

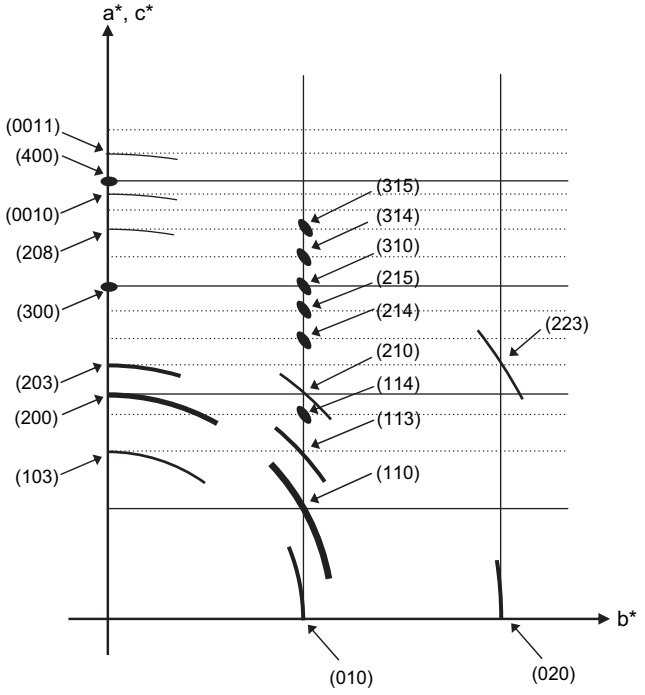


Fig. 7. Reciprocal lattice for the $a^*-c^*$ and $b^*-c^*$ net of the PLLA-TC film.

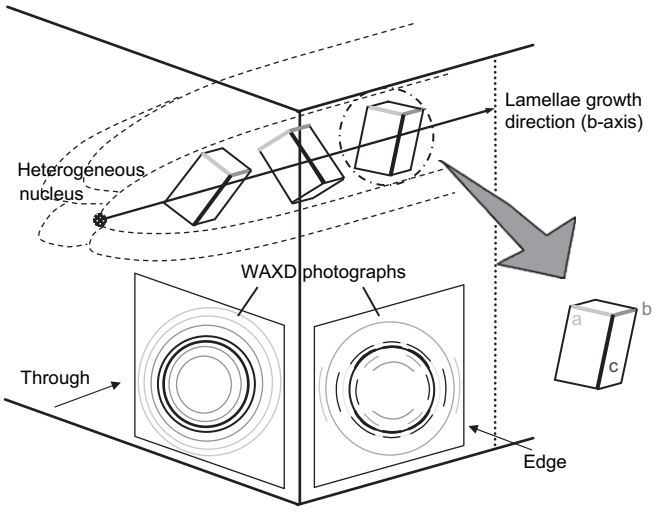


Fig. 8. The lamellar growth model of the PLLA-TC structure.

structure. The results of edge-view WAXD analysis for the TC film indicate that the *c*-axis of the PLLA unit cell orients in parallel to the film surface.

Previously, Gazzano et al. have reported that the *a*-axis lay along the radius of spherulite of PLLA [34]. However, it is also possible to perform the indexing by using reciprocal lattice pattern oriented *b*-axis as fiber axis. It may be difficult to accurately decide oriented axis in spherulite containing randomly oriented crystallites only. Since TC structure forms the definite oriented structure in this study, it is supposed that our suggestion is reliable.

Table 2
Results of WAXD for PLLA-TC film obtained at 122 °C in the edge direction

| $2\theta$/° | *d*-Spacing/Å | | *hkl* |
|---|---|---|---|
| | Observed | Calculated | |
| 12.4 | 7.14 | 7.14 | 103 |
| 14.7 | 6.03 | 6.03 | 010 |
| 16.6 | 5.34 | 5.39 | 200 |
| 16.8 | 5.28 | 5.27 | 110 |
| 19.0 | 4.67 | 4.70 | 203 |
| 19.1 | 4.65 | 4.62 | 113 |
| 20.7 | 4.29 | 4.25 | 114 |
| 22.4 | 3.97 | 4.02 | 210 |
| 24.9 | 3.58 | 3.59 | 300 |
| 24.9 | 3.58 | 3.50 | 214 |
| 27.4 | 3.26 | 3.29 | 215 |
| 29.0 | 3.08 | 3.02 | 020 |
| 29.1 | 3.07 | 3.09 | 310 |
| 31.1 | 2.88 | 2.92 | 208 |
| 31.3 | 2.86 | 2.84 | 314 |
| 32.1 | 2.79 | 2.78 | 0010 |
| 33.0 | 2.72 | 2.72 | 315 |
| 33.2 | 2.70 | 2.70 | 400 |
| 34.2 | 2.62 | 2.65 | 402 |
| 35.3 | 2.54 | 2.53 | 0011 |
| 41.5 | 2.18 | 2.26 | 415 |

To clarify the lamellar stacking mode in the PLLA-TC film, SAXS measurements were carried out. Fig. 9 displays the SAXS patterns of the PLLA-TC film in the edge and through directions. A stronger streak along the meridian direction and weaker isotropic scattering are observed when X-ray beam was incident parallel to the film surface (Fig. 9a), whereas a Debye ring appears clearly in the through view (Fig. 9b). From the edge-view SAXS pattern, the long period in parallel to the lamellae growth direction is estimated to be *ca*. 190 Å, while that perpendicular to lamellar growth direction is *ca*. 170 Å. On the other hand, the Debye ring obtained gives the long-period value as *ca*. 190 Å.

The TEM micrographs of the replica for the fractured TC film in (a) convergent region of two different TC layers and (b) innards of TC layer are shown in Fig. 10. We find the morphology where fibrillar structures lie in parallel to lamellar growth direction. Therefore, heterogeneous nucleation occurs with some neighboring nuclei along with the film surface, suggesting that the formation of TC layers is hindered by the lateral expansion and limited growth in the one dimension (thickness direction), resulting in a columnar TC layer. The fibrillar thickness of *ca*.220 Å observed in Fig. 10 corresponds to that of the lamellar crystals. In view of these results, a hierarchical model of the PLLA-TC structure is proposed as shown in Fig. 11.

### 3.3. Influence of purification on PLLA-TC morphology

The results described above suggest that the heterogeneous nucleation on PTFE substrate in as-received sample probably occurs, as proposed by Campbell and Qayyum [17]. To

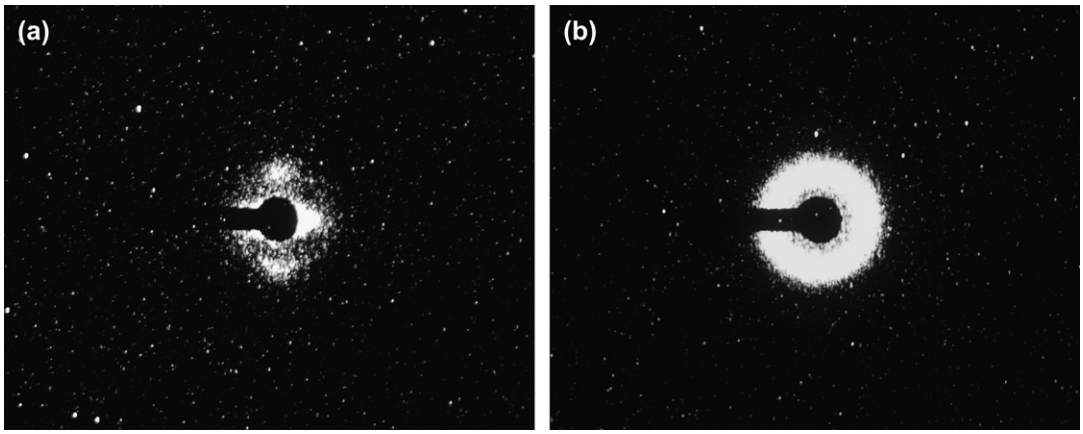


Fig. 9. SAXS photographs of the PLLA-TC film obtained at $T_c = 122$ °C in the (a) edge- and (b) through direction.

make sure the assumption, a purified PLLA sample was prepared by a process where the pellets were dissolved in chloroform, and the formation mechanism of TC structure was examined.

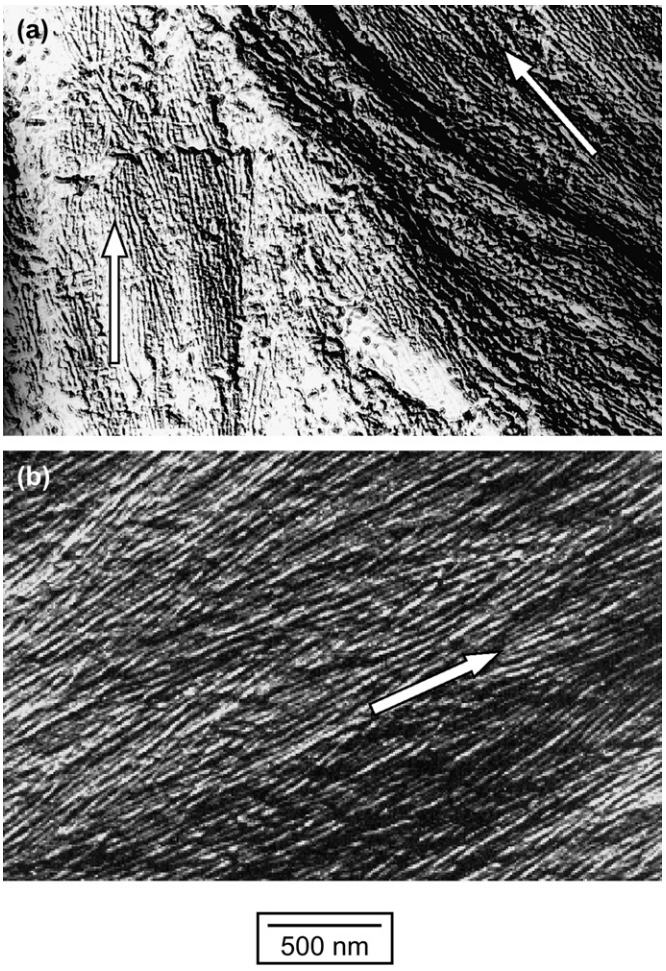


Fig. 10. Transmission electron micrographs of a cross-section replica for the PLLA-TC film obtained at $T_c = 122$ °C: (a) convergent region of two different TC layers; (b) innards of TC layer. The arrows represent lamellar growth direction.

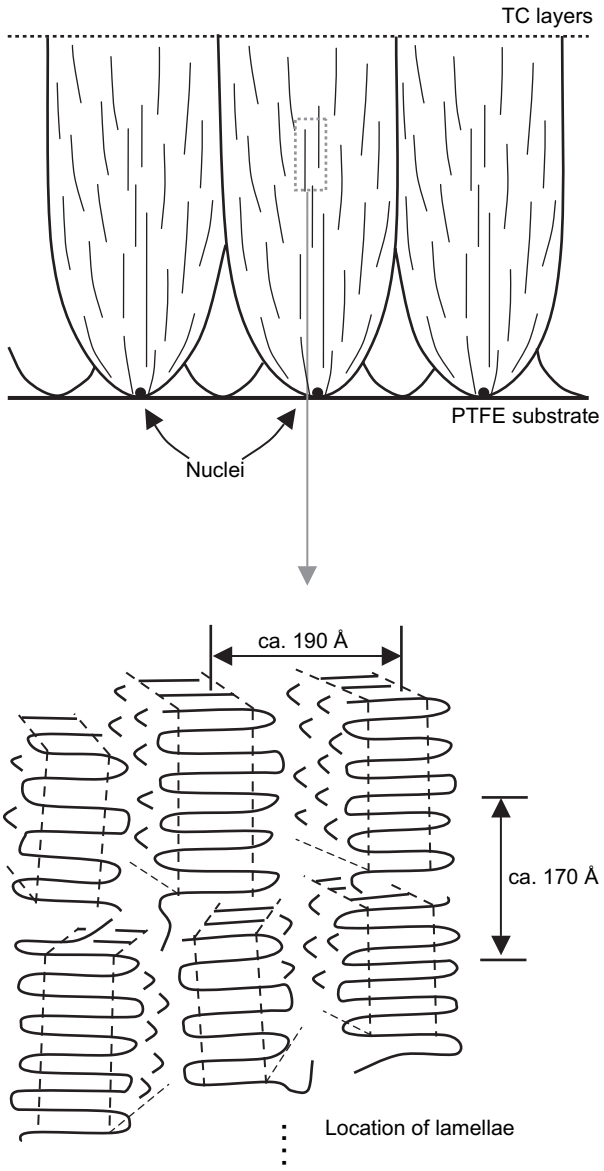


Fig. 11. The hierarchical structure model of the PLLA-TC structure.

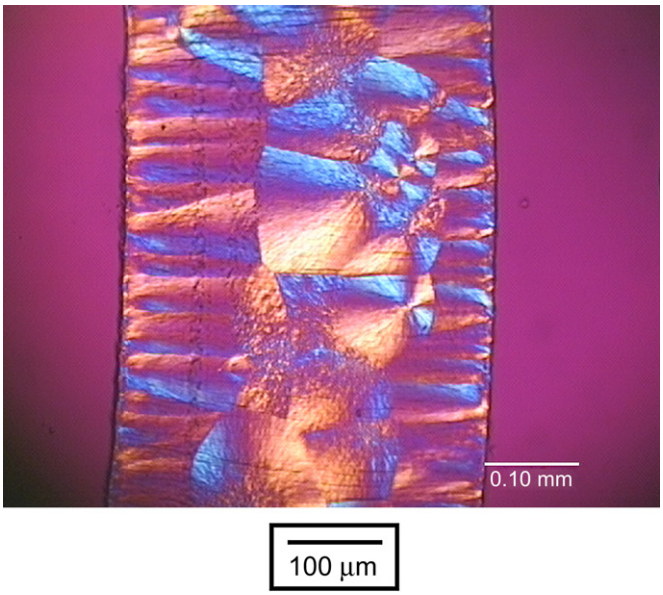


Fig. 12. Polarized optical micrographs of the purified PLLA-TC thin films at $T_c = 122$ °C in the edge direction.

Fig. 12 shows the optical micrograph of the purified PLLA-TC thin film at $T_c = 122$ °C. Obviously, well-organized TC structure disappeared in this system, while the ordinary spherulitic textures can be observed preferentially. Fig. 13 shows the DSC heating traces for the samples A and B (heating rate, 10 °C min$^{-1}$). Apparently, the value of exothermic enthalpy change ($\Delta H_c$) of the sample B is much less than that of the sample A. Additionally, in the thermograms for the sample B, the exothermic peak position shifts considerably to the higher temperature region. These results come from their growth rate on the content of relatively low molecular weight PLLA chains, which probably increase the spherulitic growth rate of $G$ as shown in Fig. 3. As reported by Miyata–Masuko [30], the $G$ value depends upon the molecular weight of PLLA, implying that low molecular weight PLLA chains were removed by the reprecipitation process.

Whether or not homogeneous nucleation occurs in the PLLA polymers is confirmed by observing the repeated isothermal crystallization at the same temperature. Fig. 14 shows the mode of spherulitic growth for the sample A and sample B at $T_c = 122$ °C for 10 min from the isotropic melt. In this case, we find that the spherulite size of sample A is larger than that of the sample B, and the number of spherulites in sample A is less than that of sample B. For sample A, it is apparent that the heterogeneous nucleation is caused by impurities in this system, since the spherulites appear in the same place. In contrast, the nucleation in a different place was sporadically caused in the purified PLLA, suggesting that it becomes a nucleus by intermolecular aggregation of the PLLA chain.

The changes in morphology with purification of PLLA samples are caused by effectual removal of the impurities such as an oxidant inhibitor and catalyst residues. Therefore, an enough nucleus density to form TC structure decreases due to insignificant adsorption of TC nuclei occurred on the PTFE surface. Concerning the well-organized TC structure, nucleation rates in the as-received samples on the PTFE surface are thus dependent on the concentration of impurity involved in sample A.

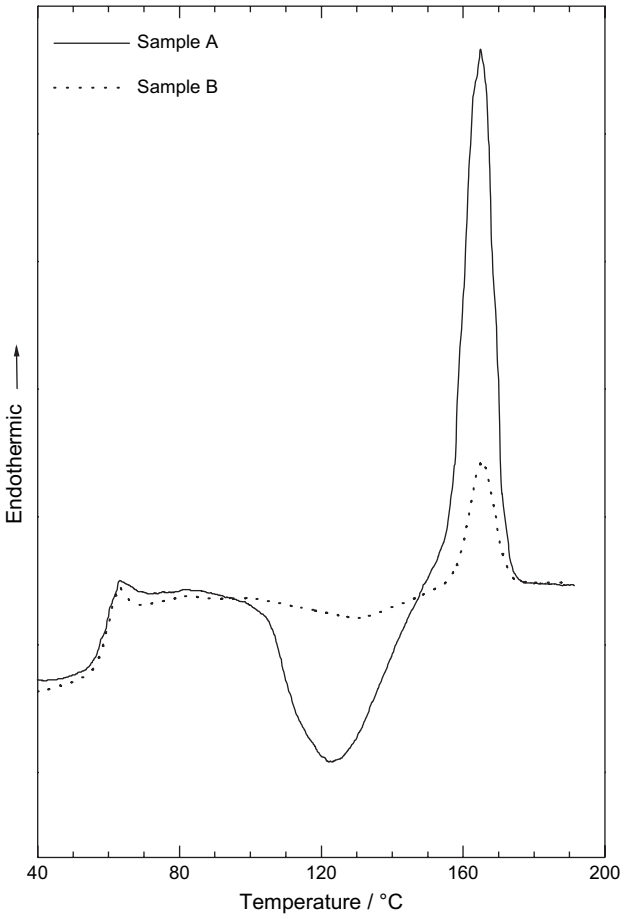


Fig. 13. DSC heating traces of the samples A (solid line) and B (dashed line). The heating rate in DSC measurement was 10 °C min$^{-1}$.

## 4. Conclusions

The PLLA film involving the TC structures was formed by higher heterogeneous nucleation on the PTFE substrates in isothermal crystallization at 122 °C. The formation mechanism of the TC structure was governed by the fact that one-dimensional lamellae are grown in the parallel direction to the $b$-axis. On the contrary, the ordinary spherulitic textures in the film were preferably observed in the purified PLLA sample with a homogeneous nucleation mode. Consequently, the formation of well-organized TC structure was due to suitable crystallization conditions, such as selection of crystallization temperature related to the maximum spherulitic rate and adequate amount of nucleating agent on the substrate.

## Acknowledgements

The authors would like to appreciate Mr. Hirokazu Kawai and Mr. Takayuki Aoyama for their experimental assistance.

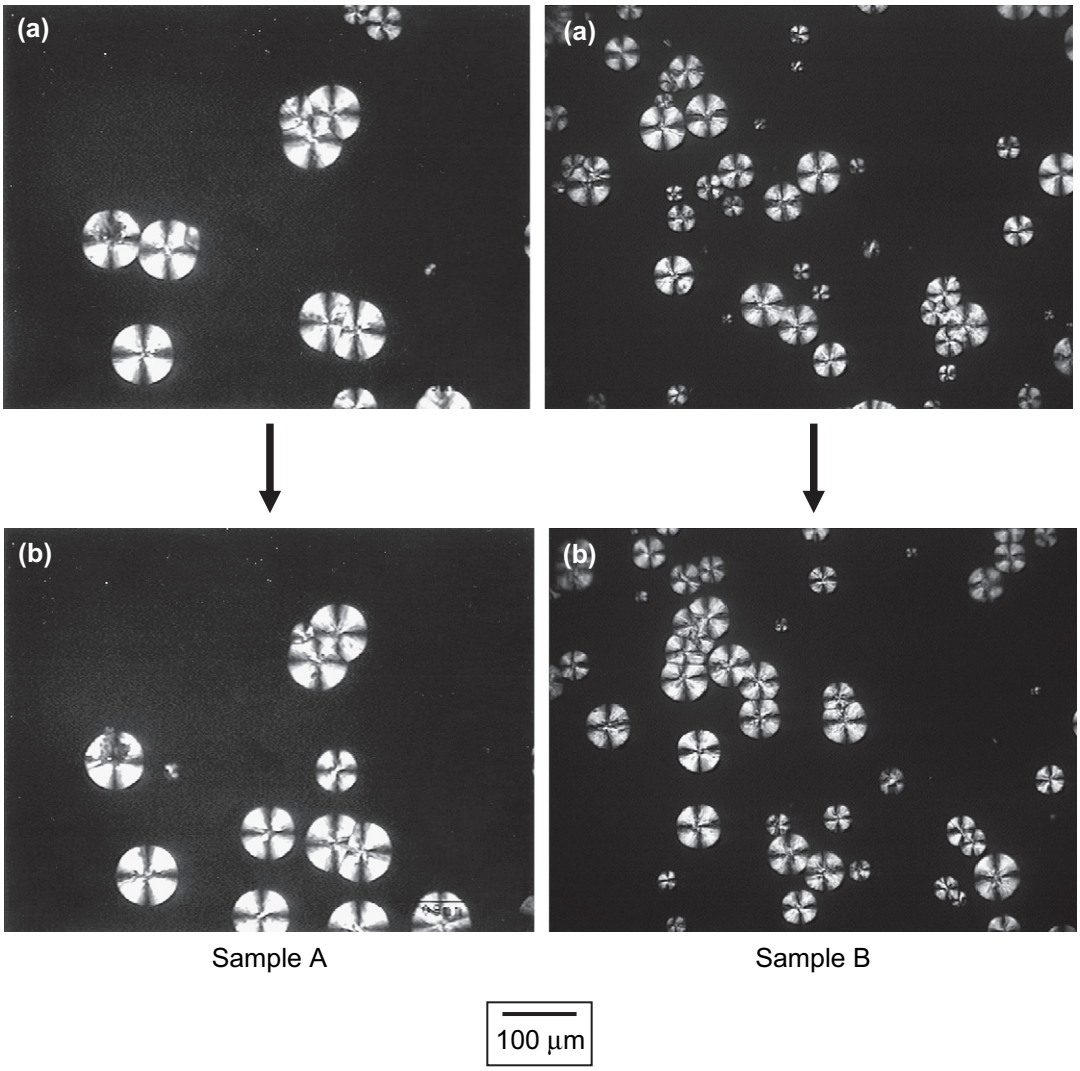


Fig. 14. Mode of spherulitic growth for the sample A and sample B at the same temperature (122 °C) for 10 min from the isotropic melt: (a) 1st run; (b) 2nd run.

## References

[1] Beck HN, Ledbetter HD. J Appl Polym Sci 1965;9:2131.
[2] Gray DG. J Polym Sci Polym Lett Ed 1974;12:645.
[3] Campbell D, Qayyum MM. J Mater Sci 1977;14:2427.
[4] Hobbs SY. Nature 1971;233:592.
[5] Hata T, Ohsaka K, Yamada T, Nakamae K, Shibata N, Matsumoto T. J Adhes 1994;45:125.
[6] Folkes MJ, Hardwick ST. J Mater Sci Lett 1987;6:656.
[7] Lee YC, Porter RS. Polym Eng Sci 1986;26:633.
[8] Tung CM, Dynes PJ. J Appl Polym Sci 1987;33:505.
[9] Wang W, Qi ZN, Jeronimidis G. J Mater Sci 1991;26:5915.
[10] Bessel T, Shortall JB. J Mater Sci 1975;10:2035.
[11] Fitchmun DR, Newman S, Wiggle R. J Appl Polym Sci 1970;14:2441.
[12] Wang C, Hwang LM. J Polym Sci Part B Polym Phys 1996;34:47.
[13] Lin CW, Du YC. Mater Chem Phys 1999;58:268.
[14] Lin CW, Ding SY, Hwang YW. J Mater Sci 2001;36:4943.
[15] Cho KW, Kim DW, Yoon S. Macromolecules 2003;36:7652.
[16] Chatterjee AM, Price FP, Newman S. J Polym Sci Part B Polym Phys 1975;13:2369.
[17] Campbell D, Qayyum MM. J Polym Sci Part B Polym Phys 1980; 18:83.
[18] Thomason JL, Vanrooyen AA. J Mater Sci 1992;27:889.
[19] Vert M, Chabot F, Leray J, Christel P. Makromol Chem Suppl 1981;5:30.
[20] Eitenmuller J, Muhr G, Gerlach KL, Schmickal T. J Bioact Compat Polym 1989;4:215.
[21] Taylor MS, Daniels AU, Andriano KP, Heller J. J Appl Biomater 1994;5:151.
[22] Park TG, Cohen S, Langer R. Macromolecules 1994;25:116.
[23] Hoogsteen W, Postema AR, Pennings AJ, ten Brinke G, Zugenmaier P. Macromolecules 1990;23:634.
[24] Kobayashi J, Asahi T, Ichikawa M, Oikawa A, Suzuki H, Watanabe T, et al. J Appl Phys 1995;77:2957.
[25] Miyata T, Masuko T. Polymer 1997;38:4003.
[26] Eling B, Gogolewski S, Pennings AJ. Polymer 1982;23:1587.
[27] Leenslag JW, Pennings AJ. Polymer 1987;28:1695.
[28] Vasanthakumari R, Pennings AJ. Polymer 1983;24:175.
[29] Kishore K, Vasanthakumari R. Colloid Polym Sci 1988;266:999.
[30] Miyata T, Masuko T. Polymer 1998;39:5515.
[31] Fukada E. IEEE Trans Electr Insul 1992;27:813.
[32] Tajitsu Y, Sukegawa M, Kikuchi M, Suto N, Kudo M, Masuko T, et al. Jpn J Appl Phys Part 1 2003;42:6172.
[33] Nakiri T, Imoto K, Ishizuka M, Okamoto S, Date M, Uematsu Y, et al. Jpn J Appl Phys 2004;43:6769.
[34] Gazzano M, Focarete ML, Riekel C, Scandola M. Biomacromolecules 2004;5:553.